



Contents lists available at ScienceDirect

Bioorganic & Medicinal Chemistry Letters

journal homepage: www.elsevier.com/locate/bmcl

SAR and characterization of non-substrate isoindoline urea inhibitors of nicotinamide phosphoribosyltransferase (NAMPT)

Michael L. Curtin^{*}, H. Robin Heyman, Richard F. Clark, Bryan K. Sorensen, George A. Doherty, T. Matthew Hansen, Robin R. Frey, Kathy A. Sarris, Ana L. Aguirre, Anurupa Shrestha, Noah Tu, Kevin Woller, Marina A. Pliushchev, Ramzi F. Sweis, Min Cheng, Julie L. Wilsbacher, Peter J. Kovar, Jun Guo, Dong Cheng, Kenton L. Longenecker, Diana Raich^a, Alla V. Korepanova, Nirupama B. Soni, Mikkel A. Algire, Paul L. Richardson, Violeta L. Marin, Ilaria Badagnani, Anil Vasudevan, F. Greg Buchanan, David Maag, Gary G. Chiang^b, Chris Tse, Michael R. Michaelides

AbbVie Inc, 1 North Waukegan Rd., North Chicago, IL 60064, United States

ARTICLE INFO

Article history:

Received 24 April 2017

Revised 1 June 2017

Accepted 4 June 2017

Available online xxxx

Keywords:

NAMPT inhibitors
Isoindoline ureas
Antitumor activity
Cancer

ABSTRACT

Herein we disclose SAR studies that led to a series of isoindoline ureas which we recently reported were first-in-class, non-substrate nicotinamide phosphoribosyltransferase (NAMPT) inhibitors. Modification of the isoindoline and/or the terminal functionality of screening hit **5** provided inhibitors such as **52** and **58** with nanomolar antiproliferative activity and preclinical pharmacokinetics properties which enabled potent antitumor activity when dosed orally in mouse xenograft models. X-ray crystal structures of two inhibitors bound in the NAMPT active-site are discussed.

© 2017 Elsevier Ltd. All rights reserved.

Nicotinamide adenine dinucleotide (NAD⁺) functions as a coenzyme for many metabolic processes and as a substrate for enzymes involved in calcium signaling, DNA repair and regulation of gene expression.¹ In its role as a substrate for enzymes including the poly(ADP-ribose) polymerases and sirtuins, NAD⁺ is consumed when its ADP-ribose unit is transferred to acceptor molecules, generating nicotinamide (NAM) in the process. While multiple pathways for NAD⁺ biosynthesis have been identified, NAM can be efficiently recycled to NAD⁺ via a two-step process involving nicotinamide phosphoribosyltransferase (NAMPT).² This enzyme catalyzes the first and rate-determining step of the sequence, namely, the condensation of NAM with phosphoribosyl pyrophosphate (PRPP) to produce the phosphoribose adduct nicotinamide mononucleotide (NMN) (Fig. 1). This phosphoribosylated product is subsequently converted to NAD⁺ by a second enzyme, nicotinamide mononucleotide adenylyltransferase (NMNAT). Cancer cells

have a unique metabolism which includes an increased dependence upon NAD⁺/NADH-driven processes (e.g., glycolysis)³ and increased NAD⁺ consumption⁴; as a result, many cancer cells are highly dependent on NAMPT-driven NAD⁺ biosynthesis for proliferation and viability.⁵ Thus, it was hypothesized that blockade of NAM-to-NAD⁺ recycling through NAMPT inhibition could represent an effective oncology treatment that would preferentially target cancer cells.^{6,7}

The first generation small-molecule NAMPT inhibitors, FK866⁸ (**1**) and GMX1778⁹ (**2**), were evaluated clinically almost ten years ago^{10,11}; these inhibitors had potent antitumor activity in mouse xenograft models but lacked sufficient oral bioavailability and failed to elicit efficacy in human cancer trials. In the past five years a number of second generation inhibitors have appeared¹² including multiple series from Forma/Genentech¹³ [e.g., **3** and **4** (GNE-617)]. The binding mode of many of these inhibitors has been verified through X-ray crystal structures^{14,15} and, prior to the work disclosed in this manuscript, all known NAMPT inhibitors with potent cellular activity possessed a heterocyclic 'cap group' that mimics the pyridyl ring of NAM and contains an sp² nitrogen that could potentially be phosphoribosylated by the enzyme. In fact, phosphoribosylation of several of these inhibitors has been observed experimentally using mass spectrometry or X-ray crystal

^{*} Corresponding author.

E-mail address: mike.curtin@abbvie.com (M.L. Curtin).

^a Current address: MPI Research, 54943 North Main Street, Mattawan, MI 49071, United States.

^b Current address: eFFECTOR Therapeutics, 11180 Roselle Street, Suite A, San Diego, CA 92121, United States.

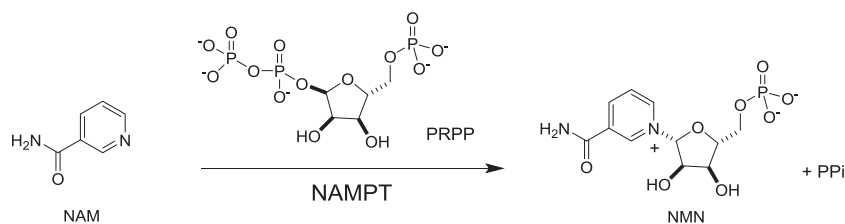


Fig. 1. The phosphoribosylation of NAM by NAMPT to provide NMN.

structures.^{15–19} These observations, along with SAR that often revealed steep losses in potency when the sp^2 nitrogen of the cap group was removed, led several groups to suggest that the ability of NAMPT inhibitors to form phosphoribosylated adducts may be necessary to obtain potent cellular activity.^{15,17}

We recently disclosed¹⁹ that during a screening effort to simultaneously identify novel anti-cancer targets and small molecules with activity against those targets, we observed a small cluster of isoindoline ureas (e.g., **5**, Fig. 2) that had potent antiproliferative activity against five of the eight cancer cell lines tested. Inhibitor affinity capture studies using a modified version of **5** as the probe revealed NAMPT as the major biochemical target; this was confirmed by biochemical assays and X-ray crystallography using human NAMPT. It was also shown that supplementation of cell culture medium with NMN, the product of NAMPT, fully restored the viability of tumor cells in the presence of high concentrations of compound **5** thus indicating that NAMPT inhibition was solely responsible for the antiproliferative activity observed with this compound. This experiment also demonstrated that an inhibitor that cannot be phosphoribosylated by NAMPT could possess potent activity against a tumor cell line. Herein we disclose the SAR and physicochemical characterization of this series of first-in-class, non-substrate, isoindoline urea inhibitors of NAMPT.

The overlaid X-ray crystal structures of isoindoline **5** (PDB ID: 5UPE) and NAM (PDB ID: 2E5D) bound in the active site of NAMPT is shown in Fig. 3. As summarized previously, the NAMPT active site consists of four distinct subsites: the hydrophilic PRPP binding site which is unoccupied by NAM (subsite A); the NAM binding space in which NAM makes important pi-stacking and hydrogen bond interactions (subsite B); the long, narrow and lipophilic tunnel which is not occupied by bound NAM (subsite C); and the distal opening of the active site which provides a large surface for hydrophobic interactions and several bound water molecules

(subsite D). Our crystallography studies determined that: the isoindoline portion of **5** overlaps the pyridyl ring of bound NAM, engaging in pi-stacking interactions with the same residues (i.e., Phe193 and Tyr18); the urea carbonyl oxygen and N-H of **5** make the same hydrogen bond interactions with Ser275 and a protein-bound water, respectively, as the carboxamide of NAM; the *para*-phenyl linker of **5** displaces several protein-bound waters and nicely fills the lipophilic subsite C; and the propylphenyl carboxamide terminus of **5** makes hydrogen bonds and hydrophobic interactions in subsite D. Comparison of this X-ray crystal structure with those of the first- and second-generation inhibitors revealed that compound **5** makes similar inhibitor-protein interactions and generally fills the same active-site space. Furthermore, this binding mode suggested to us that while certain structural features would likely be critical to activity (e.g., urea hydrogen bonds, linker length/regiochemistry), others would probably be amenable to modification such as the subsite D functionality and the isoindoline aromatic ring.

The syntheses of most of our isoindoline ureas were straightforward and applicable to high-throughput synthesis (Scheme 1). The commercially available isocyanate **6** was coupled with isoindoline to give ester **7** which could be saponified and the resulting acid coupled with a variety of primary and secondary amines to provide amides such as **8**. The use of isocyanate **9** gave the versatile aryl bromide **10** which could be coupled using transition metal chemistry to a variety of reagents to provide compounds such as pyrazole **11**. The coupling of **10** with alkenyl boronate **12** followed by hydrogenolysis gave *N*-Boc-piperidine **13** which was deprotected and coupled to a variety of carboxylic acids to give piperidinyl amides such as **14**. A more convergent approach to the piperidinyl amides is exemplified by the urea coupling of isoindoline with commercially available aniline **15** to give amide **14** after subsequent deprotection and acid coupling; this route had greater

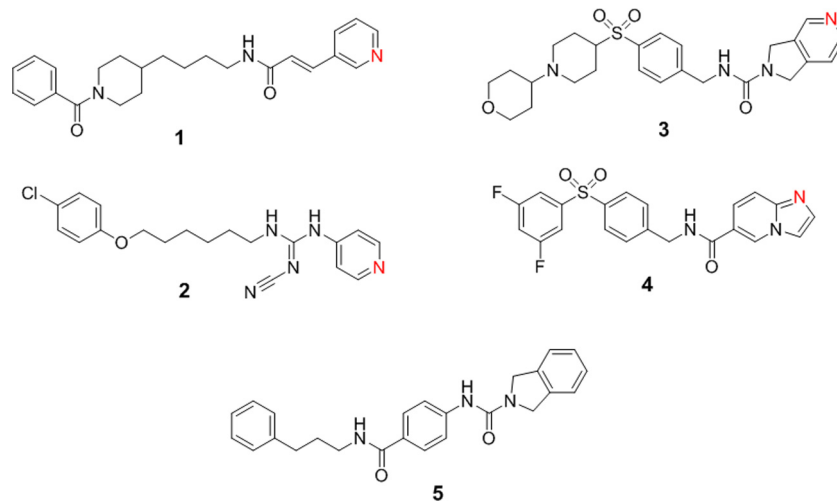


Fig. 2. NAMPT inhibitors. The sp^2 nitrogen that could potentially be phosphoribosylated by NAMPT is highlighted in red.

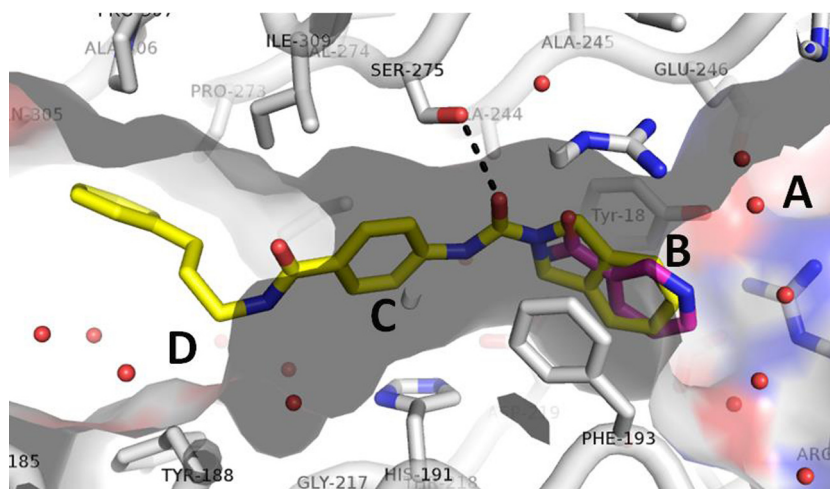
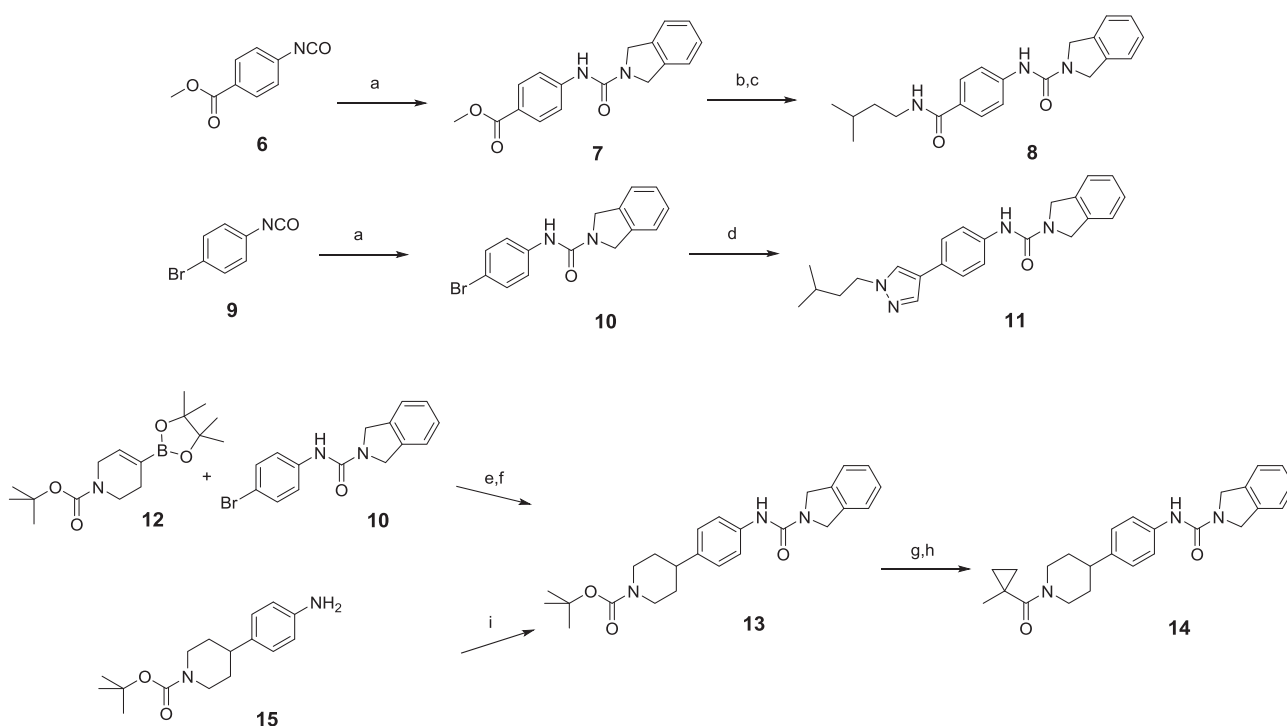


Fig. 3. Crystal structure of NAMPT complex with **5** (PDB ID: 5UPE; **5** shown as yellow sticks) with aligned overlay of NAM (PDB ID: 2E5D; NAM shown as magenta sticks). The NAMPT binding subsites (A–D) are highlighted (see text).



Scheme 1. Reagents: (a) isoindoline, THF, 0 °C then rt, 90–95%; (b) LiOH, THF/MeOH/H₂O, 96%; (c) 3-methylbutan-1-amine, EDC, HOBT, NMM, DMF, 84%; (d) 1-isopentyl-4-(4,4,5,5-tetramethyl-1,3,2-dioxaborolan-2-yl)-1H-pyrazole, PdCl₂(dppf)-CH₂Cl₂, Na₂CO₃, THF/MeOH/H₂O, 85 °C, 60%; (e) PdCl₂(dppf)-CH₂Cl₂, Na₂CO₃, THF/MeOH/H₂O, 80 °C, 74%; (f) H₂, 5% wet Pd/C, trifluoroethanol, 67%; (g) 4 M HCl in dioxane, THF, >95%; (h) 1-methylcyclopropanecarboxylic acid, EDC, HOBT, DIPEA, DMF, 95%; (i) isoindoline, bis(2,5-dioxopyrrolidin-1-yl) carbonate, pyridine, DIPEA, acetonitrile, 89%.

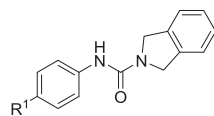
versatility and was more amenable to the multigram preparation of selected piperidinyl amide inhibitors.

New analogs were assessed for human NAMPT binding potency using a TR-FRET assay with an FK866- or isoindoline urea-based Oregon green (488) probe and for antiproliferative activity using the PC-3 (human prostate cancer) cell line. Compounds were also evaluated in a primary ADME screen that included mouse, rat and human microsomal clearance²⁰ along with microsomal protein binding, permeability and aqueous solubility. In addition, selected compounds were tested for CYP3A4 inhibition, cardiovascular liabilities, rodent pharmacokinetics (PK) and in vivo tumor inhibition in mice. Initial assessment of screening hits **5** and **8** revealed that

while these compounds had nanomolar binding affinity to NAMPT and potent, target-based antiproliferative activity (Table 1), these lipophilic compounds had no measurable bioavailability when dosed orally in mice and very low aqueous solubility (<5 μM). Aside from establishing the SAR of this series, ensuing work focused on reducing the lipophilicity of these compounds to decrease the potential for toxicity, reduce metabolic liability and increase the probability of robust in vivo activity.

The SAR work began with an examination of the alkyl carboxamide of inhibitors **5** and **8** with selected examples and two reference compounds shown in Table 1. Simplifying the terminus demonstrated that while a *para*-methyl was essentially inactive

Table 1
Initial SAR of terminal carboxamide modification and replacement.



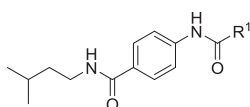
Cmpd	R ¹	NAMPT binding K _i (nM)	PC-3 cell viability IC ₅₀ (nM)	Mouse CL _{int,u,scaled} ²⁰ (L/h/kg)	Human CL _{int,u,scaled} ²⁰ (L/h/kg)	cLogP
1	FK866	3	5.7	15.5	5.5	3.0
2	GMX1778	3	4.4	81.8	34	4.1
5		9	21	NV ^a	1060	3.5
8		11	38	49	15	3.0
16	Me	2200	>10,000	NV ^a	NV ^a	2.5
17		112	2300	NV ^a	NV ^a	2.5
18		560	8000	8.9	1.2	0.8
19		104	880	4.3	3.4	2.1
20		14	21	8.7	13.0	3.4
21		160	1100	130	120	3.0
22		19	68	21	3.5	3.0
23		14	19	11	3.8	2.1
24		58	17	47	3.6	3.0
25		19	66	6.9	3.4	2.2
26		13	17	4.5	1.8	1.3
27		24	68	5.0	1.6	0.8
28		350	>10,000	265	26	3.1
11		23	32	NV ^a	NV ^a	4.0

^a Unbound intrinsic clearance could not be determined due to invalid microsomal protein binding data.

(**16**), simple carbonyls such as methyl ester (**17**) and carboxamide (**18**) were active but significantly less potent, both in binding and proliferation, than the screening hits. The *n*-propyl amide **19** regained some of the activity but the analogs with the larger alkyl groups (**5**, **8**, **20** and **22**) provided the highest potencies. Interestingly, tertiary amides such as **21** were significantly less potent than secondary amides (e.g., **20**) except if constrained in a ring as in **23**, perhaps suggesting a steric instead of an electronic explanation;

reversing the amide as in compound **24** provided a very potent subseries of inhibitors. Importantly, we determined that not only were termini bearing polar functionalities such as hydroxyl (**25**) and ether (**26**, **27**) well tolerated, they significantly increased the polarity of these compounds (as measured by clogP or logD), greatly improved oral bioavailability (e.g., see compound **58** in Table 5) and provided some of the best compounds of the isoindoline urea series (e.g., see Table 4). Lastly, replacement of

Table 2
SAR of isoindoline substitution.



Cmpd	R ¹	NAMPT binding K _i (nM)	PC-3 cell viability IC ₅₀ (nM)	Cmpd	R ¹	NAMPT binding K _i (nM)	PC-3 cell viability IC ₅₀ (nM)
8		11	38	33		4.7	>10,000
29		7.9	6.5	34		23	>10,000
30		13	10	35		16	>10,000
31		4.9	1.4	36		>9000	>10,000
32		17	640	37		7.5	8.4

carboxamide with sulfonamide (**28**) greatly diminished activity while heterocyclic replacements such as pyrazole (**11**) gave potent compounds that were highly lipophilic.

A selected summary of the effect of isoindoline substitution on activity is shown in Table 2 and demonstrates our experience that most substitution on the aryl ring were not tolerated, at least based on cellular cytotoxicity. Small substituents such as 3-fluoro (**29**) and 3-methyl (**30**) provided potent NAMPT binders with significant and robust improvement in antiproliferative activity while 3-hydroxymethyl (**31**) also gave potent analogs but usually led to inferior pharmacokinetics profiles (data not shown). 2-Chloro-substitution (**32**) attenuated cellular activity while 3-chloroisoindoline was well tolerated depending on the context (see below). Other substituents of similar size or larger such as 3-cyano (**33**), 3-trifluoromethyl (**34**) or 3-methoxy (**35**) retained active-site binding but abrogated activity in the proliferation assay; this was also true for heterocycles at the 3-position including pyridyls and pyrazoles (data not shown). Compound **36** exemplifies the fact the 3,4-disubstitution negated binding and cellular activity. Given the discussion above, it's not surprising that addition of an sp² nitrogen to the isoindoline aryl ring as in **37** provided potent binders with excellent antiproliferative activity. While a thorough comparison of several of our isoindoline and azaisoindoline ureas has been provided elsewhere¹⁹ and will not be discussed further here, it is significant that the non-substrate, 3-fluoroisoindoline ureas showed equipotent cytotoxicity with their potentially processable azaisoindoline urea comparators (e.g., **29** versus **37**). Regarding the fluorine cellular 'boost' or the lack of cellular activity with many of the isoindoline substituents, the reasons for the binding/proliferation disconnects with isoindoline substitution remain unclear.

A broad examination of the tether and terminal functionality of the isoindoline ureas was conducted and a few examples are shown in Table 3. Consistent with the description of the NAMPT

tunnel-like subsite C, the use of *meta*-substituted phenyl (**38**) eliminated binding and cellular activity as did non-linear tethers such as 2,5-furanyl and 2,5-thienyl or bulky tethers such as 1,4-cyclohexyl. The linking phenyl could be substituted with a fluoride but nothing larger and, somewhat surprisingly, 2,5- and 2–6-pyridyls were tolerated although the former (**39**) were generally more active than the latter (**40**). In addition to carboxamides, a number of terminal functionalities were well tolerated including alkyl ether (**41**) and phenyl sulfone (**42**). In contrast to sulfone **42**, the Genentech sulfone **43**²¹ was found to be inactive in our PC-3 cell viability assay; this is consistent with the Genentech antiproliferation data (IC₅₀ > 2.0 μM, A2780 cell line) and exemplifies our experience that the nature of the tether linking the isoindoline urea to the terminal functionality is a powerful determinant of potency. Because an FK-866/Abbvie hybrid molecule (**44**) that combined the alkylpiperidine benzamide with isoindoline urea proved to be very potent, we envisioned the use of phenyl-linked heterocycles (e.g., piperazine, piperidine) that would present the terminal benzamide in the same proximity as that in compounds **1** and **44**. As modeling suggested, this idea proved fruitful and while the piperazinyl linker (**45**) was not optimal, the dihydropyridine- (**46**) and piperidine-linked (**47**) benzamides were very potent inhibitors of NAMPT.

Building out the SAR of the piperidine carboxamides exemplified by **47** revealed a subseries of highly potent NAMPT inhibitors with robust binding and antiproliferative activity. The examples in Table 4 demonstrate that a wide variety of carboxamides were tolerated, ranging from lipophilic (**48**, **49**) to more polar (**50–55**), and that sulfonamides (**56**) were accommodated as well. While isoindoline substitution was not always required for optimal activity, 3-fluoro-substitution (**51**, **53**, **56** and **57**) was often used to enhance potency; we also found that 3-chloro-substitution (**55**) was beneficial in some instances. Minor changes to the linker could

Table 3
SAR of tether and terminal functionality modification.

Cmpd	Structure	NAMPT binding K_i (nM)	PC-3 cell viability IC_{50} (nM)	Mouse $CL_{int,u,scaled}^{20}$ (L/h/kg)	Human $CL_{int,u,scaled}^{20}$ (L/h/kg)	cLogP
38		>8900	>12,500	NV ^a	NV ^a	3.0
39		5.4	14	17	3.2	2.9
40		57	730	75	13	2.5
41		18	48	167	38	2.1
42		21	30	22	4.4	3.0
43		487	>10,000	220	39	3.0
44		1.6	8.4	280	19	3.6
45		19	84	NV ^a	7.8	2.6
46		3.0	8.1	NV ^a	13	2.9
47		1.0	2.8	59	11	3.0

^a Unbound intrinsic clearance could not be determined due to invalid microsomal protein binding data.

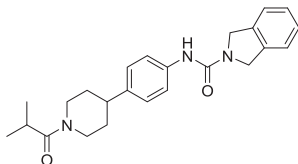
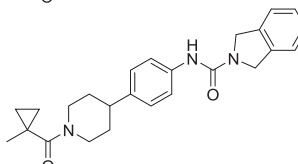
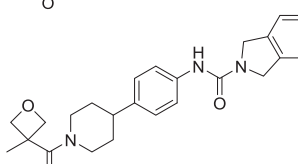
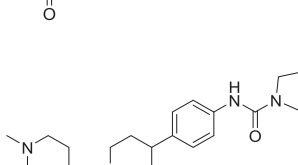
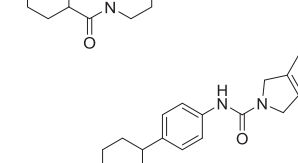
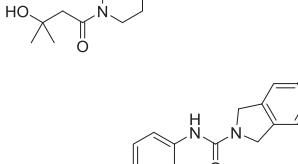
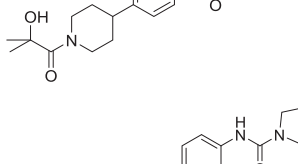
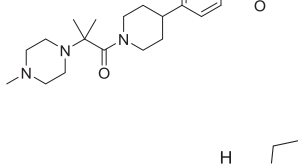
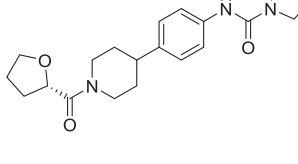
be made such as the use of azetidine as in compound **57**. While no broad link between calculated polarity (i.e., cLogP or AlogP) and unbound in vitro intrinsic clearance could be readily observed, several of these potent analogs had an optimal balance of polarity and metabolic stability that provided promising in vivo pharmacokinetics and antitumor profiles.

The X-ray crystal structure overlay of piperidine carboxamide **53** (PDB ID: 5UPF) and screening hit **5** bound in the NAMPT active site is shown in Fig. 4. As expected, the isoindoline urea of **53** makes the important pi-stacking and hydrogen bond interactions as earlier inhibitors (e.g., **5**) while the phenylpiperidine efficiently fills the lipophilic tunnel with the tertiary alcohol of the carboxamide making an interaction with a protein-bound water.

The isoindoline fluorine is oriented in an 'up' position, as shown here, which projects the halide towards Arg196 and the vacant PRPP binding site. Interestingly, this fluorine is located where the sp^2 nitrogen of the azaindoles (e.g., **37**) usually resides in the active site (data not shown), although the reasons for this overlap are not readily understood.

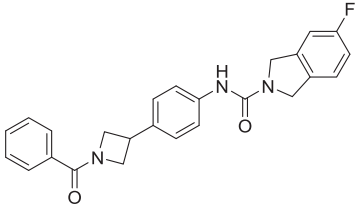
Initial analog screening based on potency, microsomal stability and permeability provided numerous promising isoindoline ureas from the various subseries that were assessed for off-target toxicities and potential drug-drug interactions (e.g., hERG blockade, in vivo rat cardiovascular effects and CYP inhibition). Selected compounds were characterized in mouse or rat pharmacokinetics studies and tested for their ability to inhibit tumor growth in a

Table 4
SAR of piperidine carboxamide modification.

Cmpd	Structure	NAMPT binding K_i (nM)	PC-3 cell viability IC_{50} (nM)	Mouse $CL_{int,u,scaled}^{20}$ (L/h/kg)	Human $CL_{int,u,scaled}^{20}$ (L/h/kg)	cLogP/AlogP
48		15	18	22	3.5	2.0/3.6
49		4.3	6.6	17	3.4	2.1/3.6
50		5.1	15	8.7	3.0	2.7/2.6
51		9.4	5.6	16	2.5	1.4/3.3
52		5.6	24	18	3.5	1.8/2.6
53		2.5	3.2	8.6	5.7	0.0/2.8
54		1.5	2.3	88	44	-0.2/3.2
55		1.7	7.9	35	13	1.1/3.4
56		3.9	6.5	30	3.5	2.5/2.9

(continued on next page)

Table 4 (continued)

Cmpd	Structure	NAMPT binding K_i (nM)	PC-3 cell viability IC_{50} (nM)	Mouse $CL_{int,u,scaled}^{20}$ (L/h/kg)	Human $CL_{int,u,scaled}^{20}$ (L/h/kg)	cLogP/AlogP
57		1.9	3.9	26	2.7	2.2/3.5

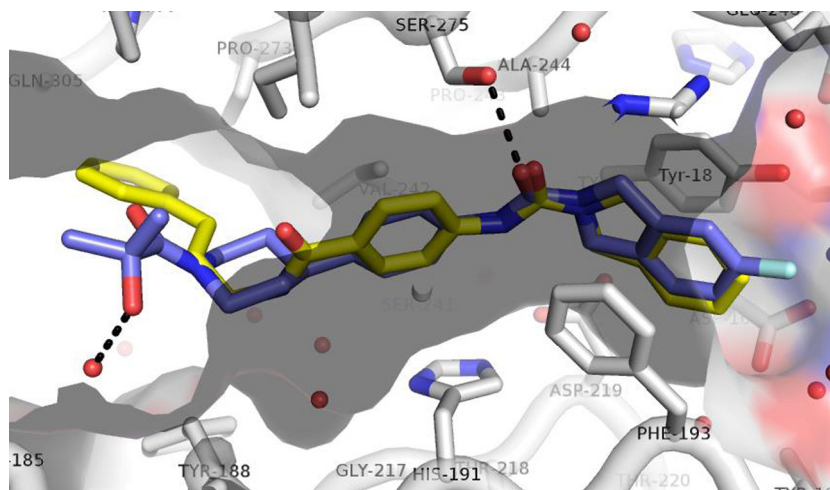
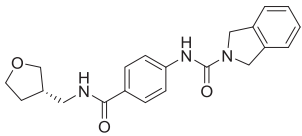
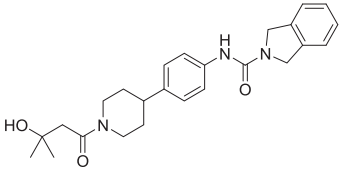


Fig. 4. Crystal structure of NAMPT complex with 5 (PDB ID: 5UPE; 5 shown as yellow sticks) with aligned overlay of 53 (PDB ID: 5UPF; 53 shown as blue sticks).

Table 5
Selected data for optimized analogs 52 and 58.

Cmpd	Structure	PC-3 cell viability IC_{50} (nM)	CYP3A4/2C9 inhibition (IC_{50} , μ M)	Rat $CL_{int,u,scaled}^{20}$ (L/h/kg)	Rat PK				%TGI (15 mg/ kg/day) ^e	Aqueous solubility (μ M)
					$t_{1/2}$ (h)	CL_p (L/h/kg)	$CL_{int,u}^{20}$ (L/h/kg)	%F		
58		56	>20/>20	<2.8	3.0 ^a	0.26 ^a	1.7 ^a	59 ^b	78%	17
52		24	16/8.4	<3.4	4.8 ^c	0.11 ^c	1.7 ^c	100 ^d	90%	3.3

^a 5 mg/kg IV dose.^b 5 mg/kg PO dose.^c 1 mg/kg IV dose.^d 1 mg/kg PO dose.^e Tumor growth inhibition in a murine xenograft model using the HCT-116 (human colorectal) cell line; compound dosed daily (3on,4off) \times 3 at given dose (mg/kg/day).

mouse xenograft model using the HCT-116 (human colorectal) cell line. Two examples, benzamide **58** (the more potent enantiomer of racemate **27**) and piperidinyl amide **52**, are shown in Table 5 with selected data. Both compounds have high oral bioavailability with low total and unbound plasma clearance in rat and provide potent antitumor activity when dosed orally in mice. Extensive experimentation revealed that the optimal dosing schedule for the isoindoline ureas was three days on/four days off per cycle which

provided maximum efficacy while minimizing toxicity.¹⁹ Inhibitors such as **58** exhibited broad in vivo anti-tumor activity across several other human tumor lines including H345 (non-small cell lung), A2780 (ovarian), ES-2 (ovarian), U87MG (glioblastoma) and H460LM (non-small cell lung).²²

In summary, we have used crystallography-driven structure-based drug design and high-throughput organic synthesis to efficiently optimize screening hit **5**, a novel non-substrate, isoindoline

urea NAMPT inhibitor. We established the SAR of these inhibitors and identified multiple analogs with potent anti-proliferative activity and vastly improved oral bioavailability. A significant number of these analogs such as isoindolines **52** and **58** provide robust antitumor activity in a mouse xenograft model after oral dosing. Further in vivo characterization of the isoindoline urea NAMPT inhibitors will be reported in the near future.

All authors are employees or former employees of AbbVie. This study was sponsored by AbbVie. AbbVie contributed to the study design, research, and interpretation of data, writing, reviewing, and approving the manuscript. The authors would like to acknowledge Stella Doktor, Patricia Stuart, Amanda Olson, Donald Osterling, and DeAnne Stolarik from the DMPK-BA Department at AbbVie for the in vitro ADME and in vivo pharmacokinetics measurements. This research used resources of the Advanced Photon Source, a U.S. Department of Energy (DOE) Office of Science User Facility operated for the DOE Office of Science by Argonne National Laboratory under Contract No. DE-AC02-06CH11357. Use of the IMCA-CAT beamline 17-ID at the Advanced Photon Source was supported by the companies of the Industrial Macromolecular Crystallography Association through a contract with Hauptman-Woodward Medical Research Institute.

A. Supplementary data

Supplementary data associated with this article can be found, in the online version, at <http://dx.doi.org/10.1016/j.bmcl.2017.06.018>.

References

- Belenky P, Bogan KL, Brenner C. NAD⁺ metabolism in health and disease. *Trends Biochem Sci.* 2007;32:12.
- Burgos ES. NAMPT in regulated NAD biosynthesis and its pivotal role in human metabolism. *Curr Med Chem.* 2011;18:1947.
- Chiarugi A, Dolle C, Felici R, Ziegler M. The NAD metabolome—a key determinant of cancer cell biology. *Nat Rev Cancer.* 2012;12:741.
- Luo J, Solimini NL, Elledge SJ. Principles of cancer therapy: oncogene and non-oncogene addiction. *Cell.* 2009;136:823.
- Mei SC, Brenner C. NAD as a genotype-specific drug target. *Chem Biol.* 2013;20:1307.
- Imai S. Nicotinamide phosphoribosyltransferase (Nampt): a link between NAD biology, metabolism, and diseases. *Curr Pharm Des.* 2009;15:20.
- Sampath D, Zabka TS, Misner DL, O'Brien T, Dragovich PS. Inhibition of nicotinamide phosphoribosyltransferase (NAMPT) as a therapeutic strategy in cancer. *Pharmacol Ther.* 2015;151:16.
- Wosikowski K, Mattern K, Schemainda I, Hasmann M, Rattel B, Löser R. WK175, a novel antitumor agent, decreases the intracellular nicotinamide adenine dinucleotide concentration and induces the apoptotic cascade in human leukemia cells. *Cancer Res.* 2002;62:1057.
- Beauparlant P, Bédard D, Bernier C, et al. Preclinical development of the nicotinamide phosphoribosyl transferase inhibitor prodrug GMX1777. *Anticancer Drugs.* 2009;20:346.
- Holen K, Saltz LB, Hollywood E, Burk K, Hanauke A-R. *Invest New Drugs.* 2008;26:45.
- von Heideman A, Berglund A, Larsson R, Nygren P. Safety and efficacy of NAD depleting cancer drugs: results of a phase I clinical trial of CHS 828 and overview of published data. *Cancer Chemother Pharmacol.* 2010;65:1165.
- Galli U, Travelli C, Massarotti A, et al. Medicinal chemistry of nicotinamide phosphoribosyltransferase (NAMPT) inhibitors. *J Med Chem.* 2013;56:6279.
- Zak M, Liederer BM, Sampath D, et al. Identification of nicotinamide phosphoribosyltransferase (NAMPT) inhibitors with no evidence of CYP3A4 time-dependent inhibition and improved aqueous solubility. *Bioorg Med Chem Lett.* 2015;25:529. and references cited therein.
- Khan JA, Tao X, Tong L. Molecular basis for the inhibition of human NMPRTase, a novel target for anticancer agents. *Nat Struct Mol Biol.* 2006;13:582.
- Zheng X, Bauer P, Baumeister T, et al. Structure-based identification of ureas as novel nicotinamide phosphoribosyltransferase (Nampt) inhibitors. *J Med Chem.* 2013;56:4921.
- Zheng X, Bauer P, Baumeister T, et al. Structure-based discovery of novel amide-containing nicotinamide phosphoribosyltransferase (Nampt) inhibitors. *J Med Chem.* 2013;56:6413.
- Oh A, Ho Y-C, Zak M, et al. Structural and biochemical analyses of the catalysis and potency impact of inhibitor phosphoribosylation by human nicotinamide phosphoribosyltransferase. *ChemBioChem.* 2014;15:1121.
- Watson M, Roulston A, Bélec L, et al. The small molecule GMX1778 is a potent inhibitor of NAD⁺ biosynthesis: strategy for enhanced therapy in nicotinic acid phosphoribosyltransferase 1-deficient tumors. 2009;29:5872.
- Wilsbacher JL, Cheng M, Cheng D, et al. Discovery and characterization of novel, orally bioavailable non-substrate and substrate NAMPT inhibitors. *Mol Cancer Ther* [in press].
- Heinle L, Peterkin V, de Morais SM, Jenkins GJ, Badagnani I. A high throughput, 384-well, semi-automated, hepatocyte intrinsic clearance assay for screening new molecular entities in drug discovery. *Comb Chem High Throughput Screen.* 2015;18:442.
- Dragovich PS, Bair KW, Baumeister T, et al. Identification of 2,3-dihydro-1H-pyrrolo[3,4-c]pyridine-derived ureas as potent inhibitors of human nicotinamide phosphoribosyltransferase (NAMPT). *Bioorg Med Chem Lett.* 2013;23:4875.
- For a detailed summary of the in vivo antitumor activity of inhibitor **58** in a broad range of tumor types, see: Buchanan, F.G. et al., in preparation.